



Feature-based Design of Bio-degradable Micro-patterned Structures

Ibrahim T. Ozbolat¹, Michelle Marchany², Joseph A. Gardella Jr.³, Frank V. Bright⁴, Alex N. Cartwright⁵, Robert Hard⁶, Wesley L. Hicks Jr.⁷ and Bahattin Koc⁸

University at Buffalo,

¹iozbolat@buffalo.edu, ²mdm37@buffalo.edu, ³gardella@buffalo.edu, ⁴chefvb@buffalo.edu, ⁵anc@buffalo.edu, ⁶hard@buffalo.edu, ⁸bkoc@buffalo.edu

⁷Roswell Park Cancer Institute, hicksjrwesley@aol.com

ABSTRACT

This paper presents a novel feature-based variational modeling to control the biodegradation process and thus material release kinetics of biodegradable micro-structures. Pattern architecture of micro-structure is varied according to the predetermined degradation profile over the micro-structure based on tissue engineering requirements. Optimum pattern architecture is generated over the micro-structure with varying geometric features and degradation kinetics. Several micro-pattern examples are provided with different patterning features (PFs) and degradation profiles, and their time based degradation profiles are calculated based on the developed biodegradation model. An experimental study of degradation process is also developed to compare a fabricated micro-structured biodegradable material to the developed computational model.

Keywords: bio-modeling, micro structures, variational modeling, tissue engineering.

DOI: 10.3722/cadaps.2009.661-671

1. INTRODUCTION

Tissue Engineering aims to regenerate tissue structures by combining cells and biomaterial to replace diseased and damaged tissues or organs [17]. One common strategy is to develop engineered scaffolds providing an optimal microenvironment for the cells to culture and develop into tissues [15]. Biodegradable polymers are used extensively in tissue engineering to fabricate micro-structures (See Fig. 1) for scaffolds supporting cell attachment and subsequent tissue regeneration [4],[9]. One of the main reasons for using biodegradable polymers which function for a temporary period, subsequently degrade and leave human body through metabolic pathways, is to eliminate the risk of complications associated with the long-term presence of foreign material [3].

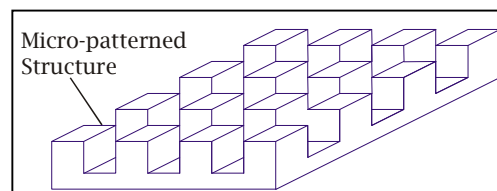


Fig. 1: A micro-patterned Structure with uniform geometry.

Controlling the degradation by varying the micro-pattern geometry could have a big impact on cell growth and proliferation such as biological response, functional and mechanical behavior, and the protein release rate. The functional behavior of the micro-structure and the amount of mechanical loading during regeneration of tissue structure change over time, and are affected by the geometry of micro-structures [6]. In addition, the micro-structure can be designed in a way to release proteins or growth factors choreographed over a time period to improve tissue regeneration while viable tissue adheres and grows into degrading construct [2]. Therefore, it is essential to release encapsulated proteins and growth factors in a controlled fashion since the incorporated proteins need to maintain their integrity to stimulate desirable cells to achieve biological response thereafter the degradation of the release system [16]. However, increasing the degradation rate deteriorates the mechanical integrity of the scaffold that is to be maintained for a period to promote cell proliferation. Therefore, controlling degradation to meet the required mechanical strength is also important [5]. In the literature, most of the studies have been conducted for the degradation analysis of biomaterials experimentally based on aforementioned properties but they take prolonged time to complete and are difficult to replicate [1], [7-8].

The major objective of this paper is to control the biodegradation process by controlling the geometry and pattern architecture of micro-pattern structures. Material release along the micro-structure is controlled by feature-based geometric modeling of micro-patterned structures and time-based cumulative material release is obtained for various micro-pattern designs.

2. FEATURE-BASED VARIATIONAL MODELING OF MICRO-PATTERNED STRUCTURES

In this research, micro-patterned structures are modeled to be used in tissue engineering to control the cellular microenvironment and allow cells to align themselves to the shape of geometrically modeled patterns. While cells proliferate through the patterns, the degradation process proceeds simultaneously leading changes in the microenvironment. To maintain appropriate microenvironment, the degradation process is to be controlled spatially and temporarily by varying micro-patterns and their geometry.

A new feature-based geometric modeling of micro-patterned structures is developed to vary and control the geometry of micro-patterns. In tissue engineering or wound healing, degradation or protein and growth factor release should change based on some predetermined profiles. This desired degradation kinetics can be represented as a function varying from one feature such as edges of a tissue or a wound to another. These features will dominate the designed pattern geometry and termed as patterning features in this paper. PFs are a collection of geometric features such as edges or points that are definable on the structure. The pattern changes from one PF to another PF over the entire structure. Variational design in micro-structures must have at least one starting PF and one ending PF to represent the variation.

2.1 Feature-based Modeling

In this paper, a micro-patterned structure M is modeled as a collection of three characteristic sets; constraints degradation profile (D) with a set of features (F) and a set of geometric constraints (C) as follows [14]:

$$\begin{aligned} D &= \{D_{\text{profile}}(u)\} & (1.1) \\ M &= (D, F, C) \\ F &= \{ \{FF_i\}_{i=0, \dots, n_i}, \{PF_j\}_{j=0, \dots, n_j} \} \in E^3 \\ C &= \{ \{C_j\}_{j=0, \dots, n_j} \} \end{aligned}$$

where E^3 is the three-dimensional Euclidean space. Degradation profile D guides the pattern variation and is modeled as a free-form curve represented by B-spline functions of parametric distance u and degree (q).

$$D_{\text{profile}}(u) = \sum_{i=0}^e N_{i,q}(u) Q_i \quad (1.2)$$

In Eqn. (1.2), Q_j are the control points that control the degradation profile. Feature set F consist of form features $\{FF_i\}_{i=0,\dots,n_i}$ and patterning features of $\{PF_j\}_{j=0,\dots,n_j}$. Form features represent the designed geometry of micro-pattern structures. As described before, patterning features dominate the starting and ending points of variation over the micro-structure. Variation in pattern is confined by set of geometric constraints $\{C_j\}_{j=0,\dots,n_j}$. Overall property Π^p including mechanical and biological behavior of the micro-structure is proportional to the degradation profile and is given in Eqn. (1.3). Two micro-structures with variation in patterns based on their degradation profiles are illustrated in Fig. 2 (a)-(b).

$$\Pi^p \approx D_{profile}(u) \tag{1.3}$$

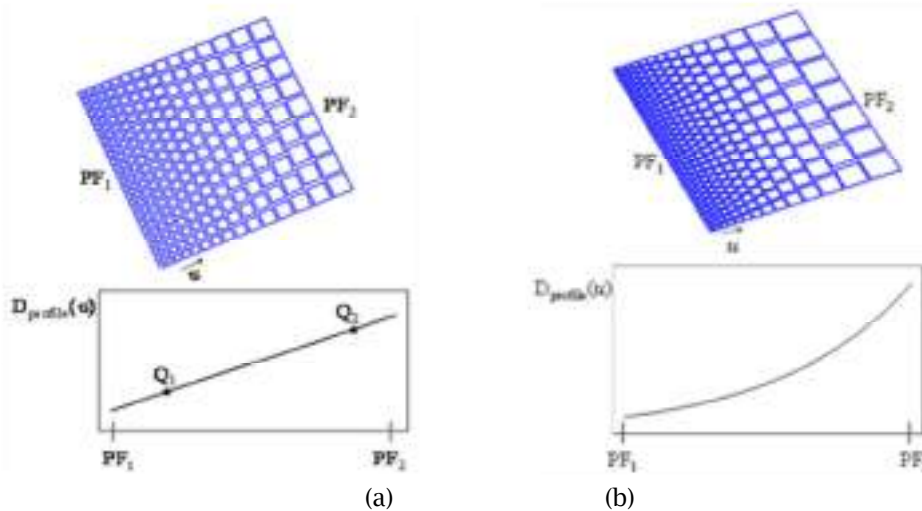


Fig. 2: Examples of micro-patterned structures with controlled geometry based on required degradation profile with (a) linear increase (b) exponential increase in degradation rate between two geometric constraints.

2.2 Geometric Variational Model: Blending

To achieve the satisfactory performance from the micro-patterned structures, the block size on the structure is varied continuously to achieve satisfactory performance. A blending (also called skinning) [12] model is proposed to represent continuous variation on degradation profile among a set of patterning feature. Patterns on the micro-structure are constrained to these patterning features and the direction of variation, which is the same as the parametric blending direction. Skinning is a process forming a surface that is a blend among a set of curves called sections curves (See Fig. 3(a)) denoted by (C_k) , where $k = 1, \dots, K$. In Fig. 3(b), curve interpolation is performed across the equally distanced control points of the section curves yielding control points (Q_i) of the blended surface where Q_i is the i th control point of i th interpolating curve $i = 1, \dots, n$. Variation of block size and location on the micro-structures is thus represented by the degradation profile that directs blending operation generating n number of interpolating curves. These curves (C_k) , called blending curves, represent the continuous variation on the geometry between two patterning features as shown in Fig. 4. Blending curves are used to separate micro-structure into uniform degradation regions. In order to generate n number of blending curves on the structure, discretization is performed on the degradation profile by dividing it into $n-1$ number of equivalent regions based on parametric distance.

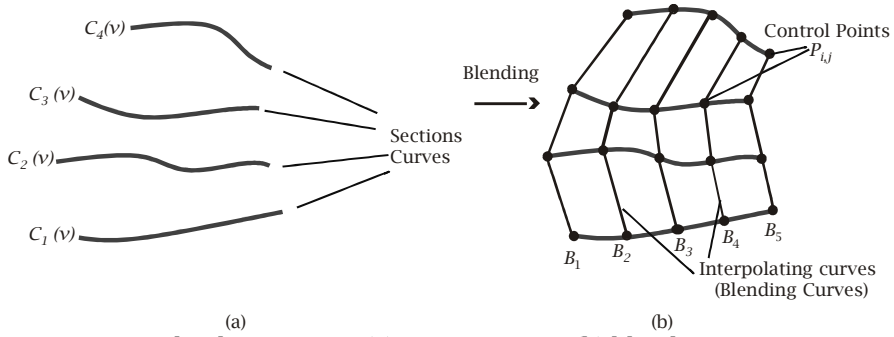


Fig. 3: Blending process (a) section curves (b) blending curves.

The value of the profile in a region is calculated with respect to the middle point of that region and is assumed to be constant everywhere in the region.

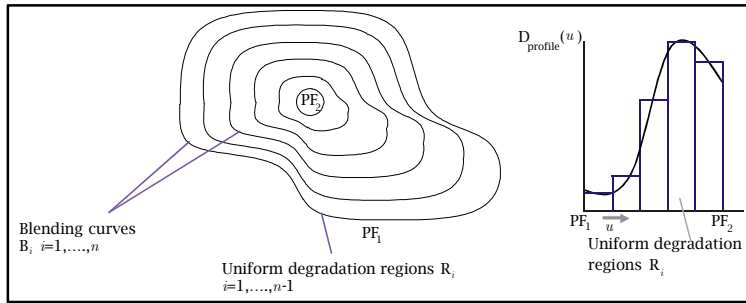


Fig. 4: Blending operation and discretization of degradation profile into uniform degradation regions between 2PFs.

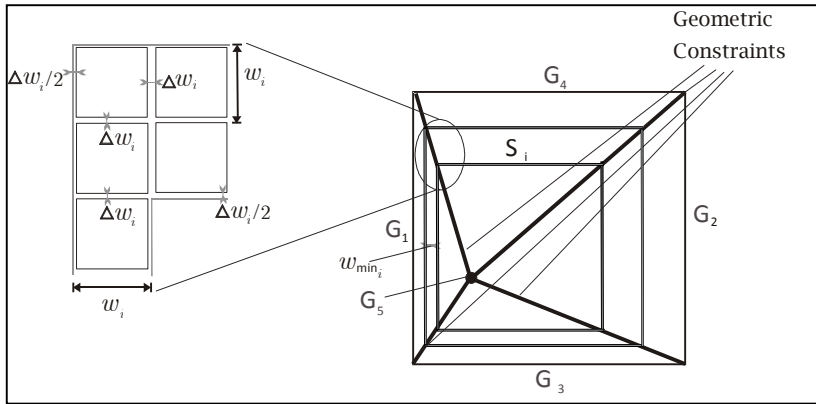


Fig. 5: Parameters for block location including region widths and the interval distances between adjacent blocks and parallel set of blocks.

While the heights of blocks are assumed to be same due to the requirement of fabrication process of micro-patterns, only change in width of block provides the variation. Total material released variation hence is performed by controlling block width. Due to the constant value of degradation profile in a region, the region encloses blocks with same width size of w_i in the corresponding region between two consecutive blending curves ($R_{i=1, \dots, n-1} = 1, \dots, K$) on the micro-structure. The value of function is

proportional to the total material released in region R_i . Micro-structures have starting and ending PFs that can be either an edge or a randomly picked point inside the structure. Each starting and ending PF couple confined within geometric constraints represents variation in the width of R_i and hence number of blocks located in this region. Width of blocks in R_i is represented as w_i . In Fig. 5, gap between two adjacent blocks along corresponding is denoted as Δw_i and it is provided initially on each sides of to locate blocks $\Delta w_i/2$ away from the related curve in order to prevent block overlap in the design. Moreover, Δw_i gap is also considered between two consecutive set of blocks in each R_i for the same reason. Smallest distance between two consecutive blending curves is denoted as w_{min_i} for each R_i .

2.3 Micro-pattern Optimization

In this section, an optimization model is developed to determine optimum size and number of blocks located in uniform degradation regions generated by the blending operation. Total number of blocks located in R_i is denoted by n_i . While the value of degradation profile is proportional to total material released in region R_i , the degradation profile is thus represented by Eqn. (3.1) in terms of corresponding block dimension and the number of blocks [10].

$$\Gamma D_{\text{profile}}(u) = w_i^2 h n_i \quad (3.1)$$

Here Γ stands for proportionality constant.

Objective:

$$\text{Minimize } w_i \quad (3.2)$$

Subject to:

$$w_i^2 h n_i - \Gamma D_{\text{profile}}(u) = 0 \quad (3.3)$$

$$n_i - \frac{A_i}{(w_i + \Delta w_i)^2} \leq 0 \quad (3.4)$$

$$w_i + \Delta w_i - w_{min_i} \leq 0 \quad (3.5)$$

$$n_i \geq 1 \forall i \quad (3.6)$$

$$w_i \geq 0 \forall i \quad (3.7)$$

$$n_i \text{ integer} \quad (3.8)$$

Here A_i is the area of R_i . The area occupied by the blocks and gaps are to be smaller than available region area, which is met by inequality constraints (See Eqn. (3.4)) in the model. In Eqn. (3.5), block size needs to be smaller than w_{min_i} so that at least one set of blocks can be located. Moreover, number of blocks should be at least 1 and integer, and width of block should be nonnegative given in Eqn. (3.6)-(3.8). Based on the aforementioned model, an algorithm is developed to locate varying blocks and obtain their degradation kinetics.

Algorithm I: Variational Micro-patterned Structures

INPUT: n = number of uniform degradation region, design constraints, gap size between blocks, PFs, $D_{\text{profile}}(u)$, uniform block height, proportionality constant.

OUTPUT: Block pattern w_i at R_i (block size and number of blocks)

- i. Get PFs, n , $D_{\text{profile}}(u)$, block height and proportionality constant.
- ii. Using Eqn. (3.3) - (3.8), calculate $w_i \forall R_i$.
- iii. While n_i is getting integer value in mathematical model, update Δw_i by Eqn. (3.9) $\forall R_i$.

$$\Delta w_i = \sqrt{\frac{A_i}{n_i}} - w_i \tag{3.9}$$

- iv. Locate blocks $\forall R_i$.
- v. Call Algorithm II for material release study based on Eqn. (3.10) developed in Ozbolat et al [10], in which a block solid domain Ω is divided into finite number of unit cells in 3-dimensional space and $M_{ijk}^{r,t}$ stands for the media concentration of a unit cell C_{ijk} at time t for increment r .

$$M_{ijk}^{r,t} \% = \sqrt{1 - e^{-\left(\frac{4}{2\sqrt{Dt}} + 0.14\left(\frac{d}{2\sqrt{Dt}}\right)^2\right) \left[\frac{3.14}{1 + 0.14\left(\frac{d}{2\sqrt{Dt}}\right)^2}\right]}} \left(\frac{M_{ijk}^{r,0}}{M_{ijk}^{r,\infty}} - 1\right) + 1 \tag{3.10}$$

Here D and d denotes the diffusion coefficient and distance from the unit cell C_{ijk} to the media boundary respectively.

To control the degradation process, a modified Finite Element Method (FEM) is developed [10]. In the proposed FEM approach, micro-patterns are divided into finite number of elements in Cartesian space. It is assumed that the micro-structure is uniformly fabricated over the entire geometry with truly amorphous regions. Diffusion of media proceeds from material boundary through inside of the structure resulting in accumulation of media in each unit cell. Media penetration through the unit cells is assumed to proceed to cell separation when media concentration of a unit cell reaches. A recursive algorithm is developed to increment time for each element until the separation of that element occurs. Once the corresponding element is detached from the micro-structure, the boundary of the structure is updated. Thus, intermediate geometry of the micro-structure and the amount of material removed for a specific time can be determined. The algorithm developed for degradation model is presented as[10]:

Algorithm II: Material Release Model

- i. Define amount of time increment and set initial percentage of media concentration $M_{ijk}^{r,t} \% = 0$ when $r = 0, \forall C_{ijk} \in \Omega$.
- ii. Discretize Ω by unit cells $C_{ijk} \in \Omega$ with unit cell dimension a . Obtain number of unit cells in x, y and z directions $(m, n, s) = \left(\frac{\text{width}}{a}, \frac{\text{height}}{a}, \frac{\text{depth}}{a}\right)$ in 3-dimensional space.
- iii. Calculate the diffusion distance from the solid boundary in x, y and z directions d_{ijk}^x, d_{ijk}^y and $d_{ijk}^z \forall C_{ijk}$ respectively.

Go to next increment by $r = r + 1$ and update $M_{ijk}^{r,t} \% , \forall C_{ijk}$ as:

$$M_{ijk}^{r,t} \% = F(d_{ijk}^x, t) \left(\frac{M_{ijk}^{r,0}}{M_{ijk}^{r,\infty}} - 1\right) + 1 \tag{3.11}$$

$$M_{ijk}^{r,t} \% = F(d_{ijk}^y, t) \left(\frac{M_{ijk}^{r,0}}{M_{ijk}^{r,\infty}} - 1\right) + 1 \tag{3.12}$$

$$M_{ijk}^{r,t} \% = F(d_{ijk}^z, t) \left(\frac{M_{ijk}^{r,0}}{M_{ijk}^{r,\infty}} - 1\right) + 1 \tag{3.13}$$

- iv. Search $\forall M_{ijk}^{r,t} \% , \text{ if } 1 - M_{ijk}^{r,t} \% < \delta$, where δ is a small number ($\delta \neq 0$), separation of C_{ijk} takes place at time t at iteration r .
- v. Generate new solid boundary and update d_{ijk}^x, d_{ijk}^y and $d_{ijk}^z, \forall C_{ijk} \in \Omega$. If all unit cells are detached from the structure when $\sum_i^m \sum_j^n \sum_k^s M_{ijk}^{r,t} \% = m \times n \times s, \forall M_{ijk}^{r,t} \%$ meeting the condition $1 - M_{ijk}^{r,t} \% < \delta$; then stop, otherwise go back to step (iii).

In this section, geometric feature based modeling of micro-pattern structures is performed by locating varying blocks optimally over the geometry and appropriate algorithms are proposed for material release study. Implementation and results of geometric feature based modeling and material release studies are presented in the next section.

3. IMPLEMENTATION AND RESULTS

For variational pattern micro-structures with different geometry and pattern architecture, functional variational pattern algorithm is implemented by using Rhino Script based on Visual Basic in Rhinoceros 4.0[13], and patterning features, micro-structure width, variational function, block height, initial sub-region width and the material type are selected by the user. Microsoft Excel Solver package is used to solve developed mathematical model. Micro-patterned structure can be designed according to needs in tissue engineering with variational block size over the micro-structures.

Fig. 6-9 illustrates 4 different micro-structure pattern architectures and based on the Algorithm I, micro-structures are designed according to the material release kinetics over the entire geometry.

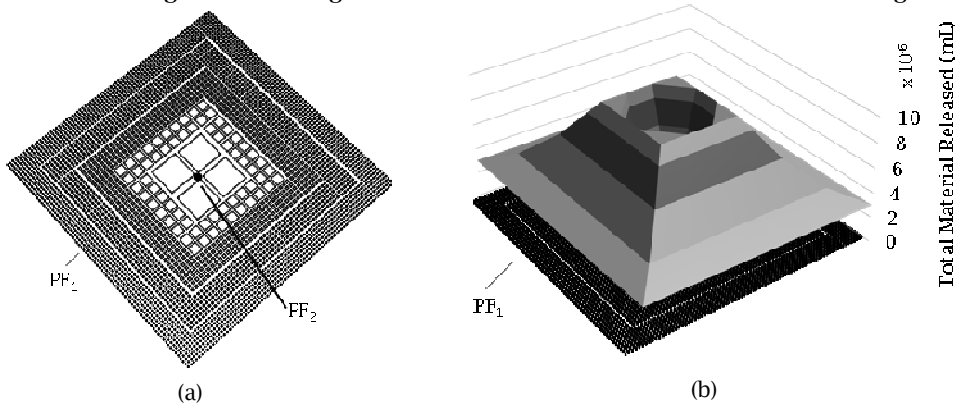


Fig. 6: Micro-structure example with 2 PFs: starting PF (4 edges) and ending PF (1 point).

In Fig. 6(a), micro-structure with 2 PFs (1 starting and 1 ending) where larger blocks are located in the middle and relatively smaller blocks are distributed along four edges. Micro-patterned structure with outer dimension 5000×5000 governed by 1PF including all available edges with $3 \times 10^{-6} mL$ total material release requirement and centre point governed by 1 PF with $0 mL$ total material release requirement is represented in Fig 6(b). According to the degradation profile requirement $D_{\text{profile}}(u) = 3 \times 10^{-6} - 17.2 \times 10^{-6} u + 82.7 \times 10^{-6} u^2 - 68.5 \times 10^{-6} u^3$ where $0 \leq u \leq 1, 5 \mu m$ height of block and $50 \mu m$ initially given gap distance, 5 uniform degradation regions are obtained. Algorithm I provides optimum block width for each region and block size over the structure increases from PF_1 to PF_2 gradually starting from $18 \mu m$ in the 1st region to $450 \mu m$ in the 5th region. In Fig. 7(a), micro-structure with 2 PFs (1 starting and 1 ending) is represented where block width increases continuously from one edge to the opposite edge. Based on requirement $D_{\text{profile}}(u) = 10^{-5} u$ where $0 \leq u \leq 1$ over $5000 \times 5000 \mu m$ structure with constant block height $5 \mu m$ and 2 PFs at two facing edges, the micro-structure is divided into 10 uniform

degradation regions and optimum number of blocks and block width in each region are obtained with initially required $50\ \mu\text{m}$ gap between blocks. Fig. 7(b) demonstrates total material released over the micro-structure with 0 at PF_1 and $10 \times 10^{-6}\ \text{mL}$ at PF_2 . Block size increases from PF_1 to PF_2 gradually with corresponding initial value of $20\ \mu\text{m}$ in the 1st region to the ending value of $447\ \mu\text{m}$ in the 10th region.

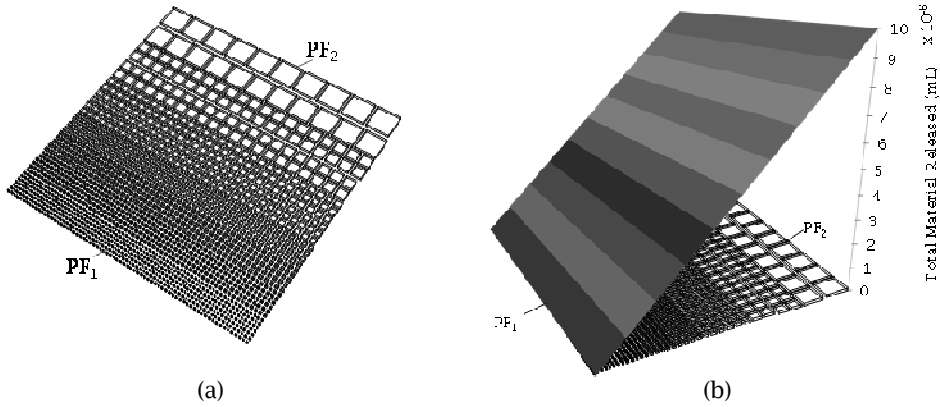


Fig. 7: Micro-structure example with 2 PFs: starting PF (1 edge) and ending PF (1 edge).

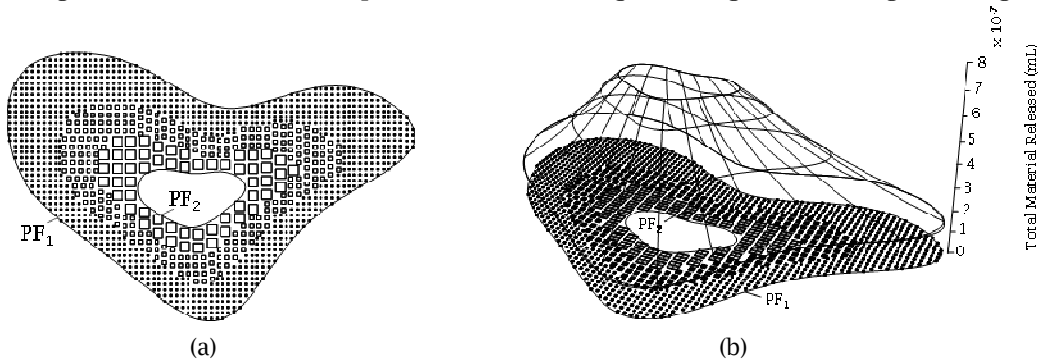


Fig. 8: Complex micro-structure example with 2 PFs: starting PF (1 edge) and ending PF (1 edge).

In Fig. 8(a), the micro-structure has a complex geometry with 2 PFs (1 starting and 1 ending) where block size increases from outer PF to inner PF confined by a hole.

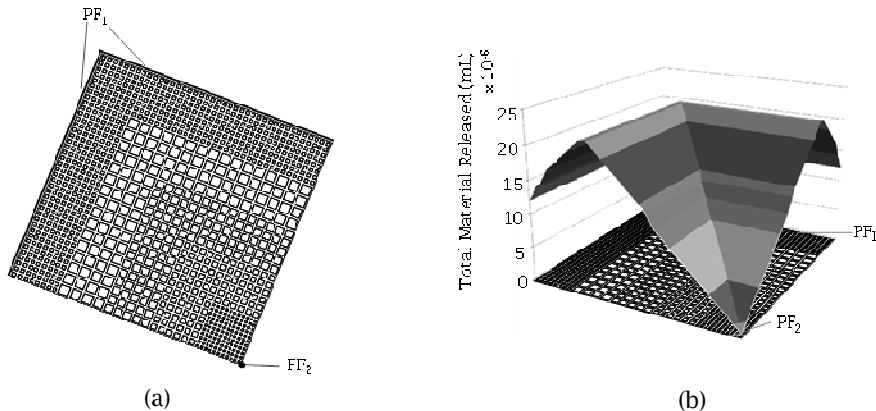


Fig. 9: Micro-structure example with 2 PFs: starting PF (2 edges) and ending PF (1 point).

In Fig. 8(b), pattern architecture on micro-structure is designed according to the requirement $D_{\text{profile}}(u) = 0.16 \times 10^{-6} + 0.92 \times 10^{-6}u - 0.35 \times 10^{-6}u^2$ where $0 \leq u \leq 1$. The structure is divided into 3 uniform degradation regions with uniform block height $5 \mu\text{m}$, $20 \mu\text{m}$ gap between blocks and block width $8.1 \mu\text{m}$, $20 \mu\text{m}$ and $48 \mu\text{m}$ in the 1st, 2nd and 3rd region respectively. The micro-structure in Fig. 9(a) is governed by 2 GFs, one is 2 adjacent edges and the other is a point located at the opposite diagonal corner. In Fig. 9(b), micro-structure is governed by 2 PFs; the starting one is 2 adjacent edges and the ending one is a point located on the opposite diagonal corner. Based on the requirement $D_{\text{profile}}(u) = 11.6 \times 10^{-6} + 74.4 \times 10^{-6}u - 174.7 \times 10^{-6}u^2 + 89.5 \times 10^{-6}u^3$ where $0 \leq u \leq 1$, uniform $5 \mu\text{m}$ block height and $50 \mu\text{m}$ gap, block widths are obtained from PF₁ to PF₂ as follows: $68 \mu\text{m}$, $196 \mu\text{m}$, $150 \mu\text{m}$, $108 \mu\text{m}$ and $41 \mu\text{m}$.

According to the material release model given in Algorithm II, time based cumulative material release study is performed for designed variational micro-patterned structures implemented in C++. The material is assumed to be polylactide(PLA) uniformly fabricated over the geometry. Fig. 10(a) shows the daily cumulative material released for the micro-structure exhibited in Fig. 7(a). Degradation and hence material release rate accelerates after 12 hours and completes totally in 30 hours.

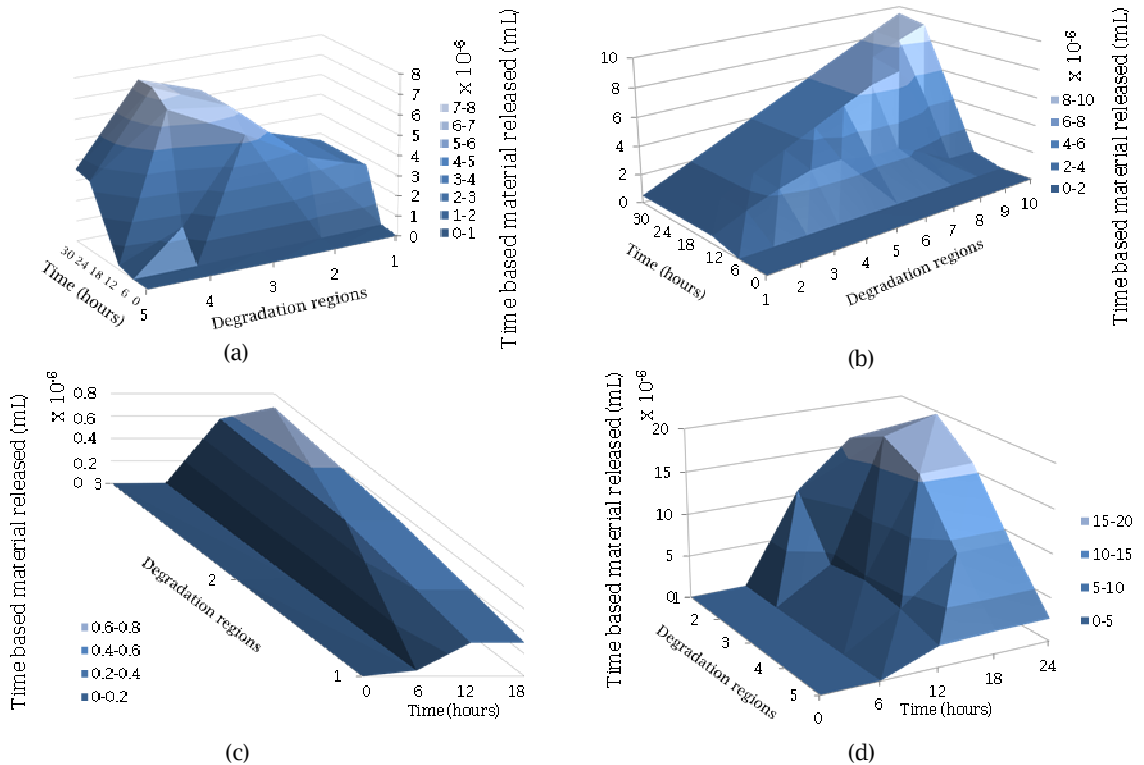


Fig. 10: Time based material release study for designed micro-structures with various degradation profiles.

In Fig. 10(b), time based cumulative material release of the micro-structure is illustrated in Fig. 8(a). Material release rate is low initially but increases after the first 6 hours, and completes in 30 hours. Material release study represented in Fig. 10(c) shows the total material release of the micro-structuredisplayed in Fig. 8(a), in which degradation process completes in 18 hours in 3 uniform degradation regions. In Fig. 10(d), degradation study of themicro-structure given in Fig. 9(a) is

represented. Release rate is closed to 0 initially, increases after 12 hours and degradation stops in 24 hours.

Top and side view of the developed simulation of biodegradation process is shown in Figure 5(a) for a single Poly-lactic Acid (PLA) block with dimensions $42 \times 42 \times 42 \mu\text{m}$. The degradation process is totally completed in 42 hours. Three dimensional intermediate geometry of degraded block with 6 hours time increments is shown in Figure 11(b).

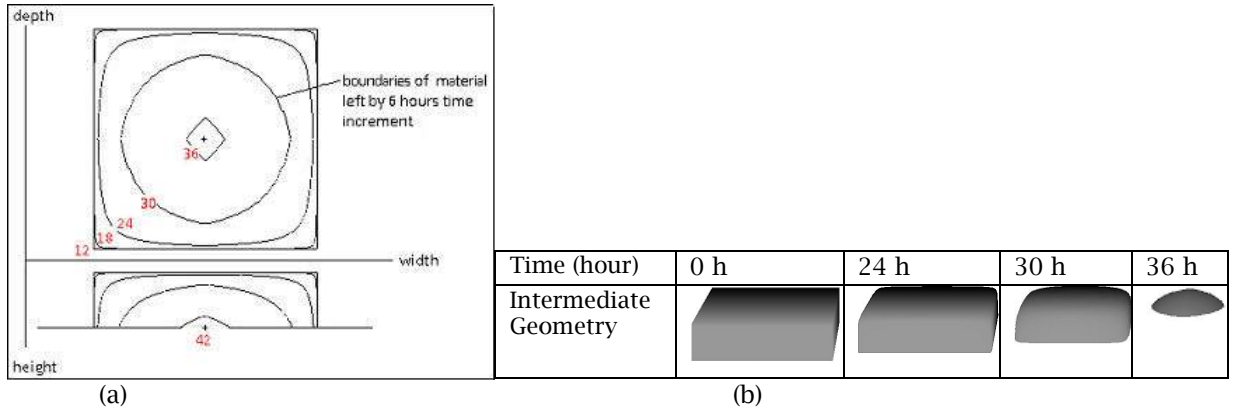


Fig. 11: (a) top and side view of a degradation process simulation based on 6 hour time increments (b) 3D view of the intermediate geometry of $42 \mu\text{m}$ degraded block [11].

A sample micro-patterned structure is fabricated to compare the fabricated micro-patterned biodegradable structure with the developed computational model (shown in Figure 11) using experimental studies. First, micro-patterned photolithographic master ($200 \mu\text{m}$ in width and $5 \mu\text{m}$ in height for this paper) was fabricated for casting of polydimethylsiloxane (PDMS) mold. Poly(D,L-lactic acid; PLA) biodegradable material was then dissolved in chloroform to make a 12% w/v solution and agitated using a mechanical shaker until dissolved. PLA solution aliquots were poured onto the PDMS mold to make micro-patterned films. The films were left to air-dry overnight and placed on a vacuum oven at room temperature.

Micro-patterned PLA films were then treated in vials with pH 7 potassium phosphate buffer solution for 3 days. The vials were submerged in a recirculating water bath at 37°C . After the degradation period, the films were rinsed with triply distilled water and dried overnight in a vacuum oven at room temperature. Micro-patterned films were analyzed using a differential interference contrast microscope (DIC) with 5X and 10X dry objective lenses. The image of the actual micro-patterned film (Figure 12(a)) and the degradation result is shown in Figure 12(b) after 3 days.

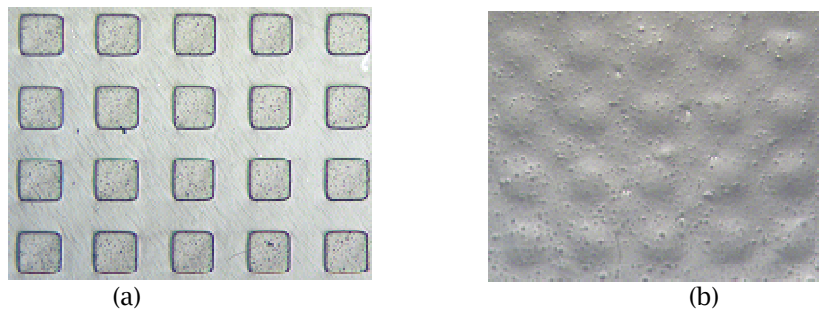


Fig.12: (a) DIC image of the fabricated micro-patterned structure with $200 \times 200 \times 5 \mu\text{m}$ patterns, (b) degraded micro-patterned structure in pH 7 potassium phosphate buffer solution for 3 days [11].

4. CONCLUSION

In this paper, a feature-based variational modeling is proposed to control the degradation kinetics of micro-patterned structures by varying the geometry and pattern architecture. Material and protein release rates during the degradation of micro-structures can be controlled by controlling the geometry of patterns on the film to fulfill the variational cell growth and proliferation in tissue engineering. Future based variational modeling in micro-patterns provides a tool to design micro-structures based on tissue engineering requirements. By enabling desired degradation profile over the entire structure governed by geometric features and constraints, optimum block size distribution is obtained over the micro-structure. Thus, required degradation kinetics over the structure is accomplished by varying the geometry and the architecture of the micro-structure by meeting desired degradation rates spatially. In this paper, proposed material release model provides a time based degradation tool extracting total material released in each predetermined time intervals. For future work, optimum design of complex structures' variational geometries can be modeled based on material release kinetics needs in tissue engineering.

5. REFERENCES

- [1] Agrawal, C. M.; McKinney, J. S.; Lanctot, D.; Anhanasiou, K. A.: Effects of fluid flow on the in vitro degradation kinetics of biodegradable scaffolds for tissue engineering, *Biomaterials*, 21(23), 2000, 2443-2452.
- [2] Anderson, J.; Rosenholm, J.; Linden, M.: Mesoporous silica: An alternative diffusion controlled drug delivery system, In: Ashammakhi, N. (ed.): *Topics in Multifunctional Biomaterials & Devices*, University of Oulund, Finland, 2008.
- [3] Bostman, O.; Pihlajamaki, H.: Clinical biocompatibility of biodegradable orthopedic implants for internal fixation: a review, *Biomaterials*, 21(24), 2000, 2615-2621.
- [4] Boucard, N.; Vitona, C.; Agayb, D.; Maric, E.; Rogerc, T.; Chancerelleb, Y.; Domard, A.: The use of physical hydrogels of chitosan for skin regeneration following third-degree burns, *Biomaterials*, 28(24), 2007, 3478-3488.
- [5] Davis, M. E.; Hsieh, P. C.; Grodzinsky, A. J.; Lee, R. T.: Custom design of the cardiac microenvironment with biomaterials, *Circ. Res.*, 97, 2005, 8-15.
- [6] Gomez, C.: *A Unit Cell Based Multi-scale Modeling and Design Approach for Tissue Engineered Scaffolds*, Drexel University, Princeton, NJ, 2007.
- [7] Kang, Y.; Xu, X.; Yin, G.; Chen, A.; Liao, L.; Yao, Y.; Huang, Z.; Liao, X.: Comparative study of the in vitro degradation of poly (L-lactic acid)/ β -tricalcium phosphate scaffold in static and dynamic simulated body fluid, *European Polymer Journal*, 43(5), 2007, 1768-1778.
- [8] Lu, L.; Peter, S. J.; Lyman, M. D.; Lai, H. L.; Leite, S. M.; Tamada, J. A.; Uyama, S.; Vacanti, J. P.; Langer, R.; Mikos, A. G.: In vitro and in vivo degradation of porous poly (DL-lactic-co-glycolic acid) foams, *Biomaterials*, 21(18), 2000, 1837-1845.
- [9] MacNeil, S.: Biomaterials for tissue engineering of skin, *Materialstoday*, 11(5), 2008, 26-35.
- [10] Ozbolat, I. T.; Marchany, M.; Bright, F. V.; Cartwright, A. N.; Gardella Jr, J. A.; Hard, R.; Hicks Jr, W. L.; Koc, B.: Feature Based Bio-Modeling of Micro-patterned Structures for Tissue Engineering, *Computer-Aided Design* (Submitted).
- [11] Ozbolat, I. T.; Marchany, M.; Gardella Jr, J. A.; Bright, F. V.; Cartwright, A. N.; Hard, R.; Hicks Jr, W. L.; Koc, B.: Computer-aided Bio-modeling of Micro-patterned Structures for Tissue Engineering, *Proc. of Industrial Engineering Research Conference*, 2009 (to appear).
- [12] Piegl, L.; Tiller, W.: *The NURBS book*, Springer 1997.
- [13] Rhinoceros 4.0, <http://www.rhino3d.com>, Robert McNeel and Associates.
- [14] Samanta, K.; Koc, B.: Feature-based design and material blending for free-form heterogeneous object modeling, *Computer-Aided Design*, 37(3), 2005, 287-305.
- [15] Starly, B.; Lau, W.; Bradbury, T.; Sun, W.: Internal architecture design and freeform fabrication of tissue replacement structures, *Computer-Aided Design*, 38(2), 2006, 115-124.
- [16] Tessmar, K. J.; Gopferich, A. M.: Matrices and scaffold for protein delivery in tissue engineering. *Advanced Drug Delivery Reviews*, 59(4-5), 2007, 274-291.
- [17] Tsang, V. L.; Bhatia, S. N.: Three-dimensional tissue fabrication. *Advanced Drug Delivery Reviews*, 56(11), 2004, 1635-1647.